Chemical Engineering Communications

ISSN: 0098-6445 (Print) 1563-5201 (Online) Journal homepage: https://www.tandfonline.com/loi/gcec20

A Novel Machine Vision Based Image Analysis Method for the Analysis of Mixing Elements in Rotary Drums

T. Koiranen, T. Melanen, J. Ilonen, T. Eerola, L. Lensu & H. Kälviäinen

To cite this article: T. Koiranen, T. Melanen, J. Ilonen, T. Eerola, L. Lensu & H. Kälviäinen (2017) A Novel Machine Vision Based Image Analysis Method for the Analysis of Mixing Elements in Rotary Drums, Chemical Engineering Communications, 204:8, 982-989, DOI: 10.1080/00986445.2017.1330746

To link to this article: https://doi.org/10.1080/00986445.2017.1330746

Published online: 21 Jun 2017.

Chemical Engineering Communications, 204:982–989, 2017

ISSN: 0098-6445 print/1563-5201 online
DOI: 10.1080/00986445.2017.1330746

A Novel Machine Vision Based Image Analysis Method for the Analysis of Mixing Elements in Rotary Drums

T. KOIRANEN[1], T. MELANEN[1], J. ILONEN[2], T. EEROLA[2], L. LENSU[2], and H. KÄLVIÄINEN[2]

[1]*LUT Chemtech, Lappeenranta University of Technology, Lappeenranta, Finland*
[2]*Machine Vision and Pattern Recognition Laboratory, Lappeenranta University of Technology, Lappeenranta, Finland*

Mixing performance in continuous rotary drums has been studied. The video analysis method was developed to evaluate different configurations of straight lifters in the rotary drum. The method converts a captured video into a single image, called stack image. The color marker tracking was estimated based on the color saturation of the stack image. Coefficients of variation and mixing indices were calculated from the color saturation profiles for different straight blade lifter configurations. The video analysis method was confronted to the impulse response of acid concentrations in water solutions. The developed analysis method has been superior with viscous fluids compared to traditional tracer impulse method in mixing evaluations. Water and 1% CMC-water solution were used in this mixing study for covering broadly different viscous materials. The drum lengthwise results for one lifter configuration were obtained from a single experiment due to the block representation of the image analysis method. It enables mixing analysis of axial segments and interaction analysis of mixer configurations. Thus, the axial mixing can be studied in more detail with rotary drums. The increase of lifters, residence time, and tip speed improved axial mixing in the studied experimental setup.

Keywords: Bioprocess engineering; Imaging; Mixing; Residence time distributions; Rheology; Rotating flow

Introduction

A large variety of rotary drums are traditionally found in different industrial operations like processing cement, lime, gypsum, and roasting of ores. Continuous rotary drums are used especially for very slow chemical or biochemical reaction kinetics where long residence times with sufficient homogenization characteristics are needed. They require low mixing power due to the low rotational speeds especially for viscous slurries (Ghorbanian et al., 2014). They are also used in homogenization of powders, and in different drying processes (Porter et al., 1973). Besides traditional drum applications, novel applications can be found as bioreactors or organic waste composters (Kalamdhad and Kazmi, 2008; Alam et al., 2009).

Address correspondence to T. Koiranen, LUT Chemical Technology, Lappeenranta University of Technology, Skinnarilankatu 34 FI-53851, Lappeenranta, Finland. E-mail: tuomas.koiranen@lut.fi

Color versions of one or more of the figures in the article can be found online at www.tandfonline.com/gcec.

Rotary drums are used not only for solids but also for liquid-based bioprocesses where low shear is favored (Sajc et al., 2000). Special interest in rotary drums can be found in organic chemicals like gluconic acid production (Šantek et al., 2006). Jiang et al. (2005) have used rotary drums in fermentation studies of by-product stream of a food process, and Jin et al. (2010) studied rotary drums for the bioleaching processes using water and dilute slurries.

The rheological properties of these bioprocess streams have a large variation depending on application, processing time, and concentration. Fermentation broth (Riley at al., 2000), anaerobically digested wastes (Mbaye et al., 2014), primary and secondary sludges (Moeller and Torres, 1997) are mainly pseudoplastic or Herschel-Bulkley rheologies. The typical apparent viscosities are from water-like fluids to 1–30 Pas at shear rate region 1–200 1/s.

Homogenization measurement methods of rotary drums have been described by Pernenkil and Cooney (2006). The invasive monitoring is based on sampling, and the non-invasive monitoring is based on, for example, magnetic resonance, positron emission, near infrared or image analysis in case of powder mixing.

The analysis methods of the mixing results are typically based on the dispersion coefficients (Sherrit et al., 2003), coefficient of variations (Poole et al., 1964), or segregation indices (Weinekötter and Reh, 1995). The basis in the mixing research has been the residence time distribution measurement. Bongo

Njeng et al. (2015a; 2015b; 2016) determined residence time distributions for different type of solids by monitoring the outlet flow NaCl concentration in the continuous flow rotary kiln equipped with longitudinal lifters. Despite the possibility of NaCl segregation, they proposed rotary drum mixing analysis based on the calculated axial dispersion coefficients for kiln slope, dam height, and number of mixing elements in the drum. Axial dispersion coefficients were 1–20 cm^2/min at rotational speeds 2–12 rpm. Gao et al. (2013) determined residence time distributions in a rotary calciner by manual image analysis for different shaped solid materials. Axial dispersion coefficients were 1–8 cm^2/min at rotational speeds 2–5 rpm.

Image-based measurements and image analysis have been used to analyze mixing behavior. In addition to this non-invasive measurement technique, these simple and low-cost methods would generally require analysis method standardization (Liu et al., 2015). An image analysis technique has been used for the analysis of transverse mixing in a 570 mm diameter and a 50 mm depth rotary drum by Van Puyvelde et al. (1999). They analyzed pixel colors and determined the mixing based on this data. The rotational speeds were from 5 to 15 rpm. The homogenization was complete under 1 min in all mixing experiments. Cabaret et al. (2007) have analyzed mixing times using color tracers and image processing in stirred tanks. Their method was based on the conversion of bitmaps into RGB pixel matrix, and the pixel separation was done using a threshold value for the red color. The mixedness value was calculated from the ratio of red pixels and from the total number of pixels in the image. Olaofe et al. (2013) have developed an image analysis technique for color classification of particles. They converted RGB images into Hue Saturation Value (HSV) color space that was used for particle identification based on their color. The application was fluidized bed segregation analysis. The method was not compared with other experimental methods. Karali et al. (2016), Liu et al. (2013), Liu et al. (2015), and Santos et al. (2016) applied image analysis for transverse mixing analysis unlike axial mixing analysis in this study.

In this research, different straight blade lifter configurations have been studied based on the measured residence time distributions for water and pseudoplastic carboxymethyl cellulose (CMC) solution simulating a large fluid viscosity range of bioprocess streams. A new video analysis method for the axial mixing measurement of residence time distributions based on stack images was developed, which is a novel approach compared to reported image analysis methods in this field. The tracer fluid test was used for the comparison of the video analysis. The analysis of the tracer fluid experiments was based on the residence time distributions of the impulse response. The method was applied for comparing mixing efficiencies of different lifter configurations in a pilot rotary drum. One major advantage of the proposed video analysis method is that it enables the analysis of residence time distribution at multiple mixing zones at once. In the experimental part of the work, the rotary drum was divided into a series of longitudinal mixing element blocks throughout the drum where individual residence time distributions were determined. The video analysis method in case of high viscous media showed its superiority compared to traditional acid tracer fluid experiments.

Materials and Methods

Materials

Water (viscosity at 20°C 1 mPas) and 1% CMC solution (Finnfix 50000 by CP Kelco) were used in this mixing study for covering broadly different viscous materials. The non-Newtonian viscosity was determined using Anton Paar Modular Compact Rheometer 302 assembled with an open cup (CC27/T200/Al) and a stirrer (ST24-2D/2 V/2 V-30/109) at shear rate region 2–100 1/s. The viscosity data as a function of shear rate was fitted using

$$\mu = K\dot{\gamma}^{n-1} \tag{1}$$

where parameters K is 27.074 and n is 0.301.

Water runs were done using HNO_3-water solution (pH 1) as an acid tracer. Blue color (color nr. 202805 from Oy Robert's Ab) was used as the color dye.

Pilot-Scale Rotary Drum

The in-house made polyacrylate pilot-scale rotary drum geometry (diameter 300 mm, total length 1150 mm, and 2.5° horizontal angle of the drum) is presented in Figure 1. The Froude numbers in the experiments were 0.00067 and 0.0027. The fluid volume inside the drum was 0.01 m^3, and the linear flow velocities 0.001 m/s and 0.002 m/s were controlled with rotameter (Fisher Porter) in case of water experiments. Linearized flow rates were controlled with manual mass flow measurements for CMC solution runs. The effective length of the mixer zone was 580 mm; the horizontal distance between mixer elements was 20 mm; the length and height of the straight blade lifters were 130 mm and 10 mm, respectively. Lifters were positioned at 90° angle to the wall. A stabilization zone of 285 mm was used in the feed and at the discharge end. Mixing configurations were varied by changing the number of lifters (0, 2 4, and 8) on 4 perimeters in the drum. A rotor pump (Zuwa Nirostar A) was used in the feed flow. A high-definition video camera, Canon Legria HFR47 (1980 × 1080 pixel), was used in the video recording at 25 frames/s, and a pH-meter (Schott CG840) was used in the acid concentration measurements. An in-house video analysis program implemented in MATLAB was used for tracking color marker. The method is described in more detail in section Video Analysis Method Based on Color Saturation.

Methods

The impulse response method (Levenspiel, 1999) was used in the analysis of the mixing in the rotary drum. In water experiments, the acid tracer was applied, and, in the case of CMC solutions, the color tracer was used.

Impulse Response Method

The impulse response method in the rotary drum has been used to study mixing for water experiments. As the acid tracer, 150 ml of HNO_3 with pH 1 was chosen. Acid was fed at the feed end as fast as possible by using the same feed position in each experiment. The pH of water solution was measured in 15 s intervals during 1800s with the pH-meter. The pH-meter was installed 850 mm from the drum feed at the centerline, and the height below the liquid surface was 50 mm. The sensor location was selected

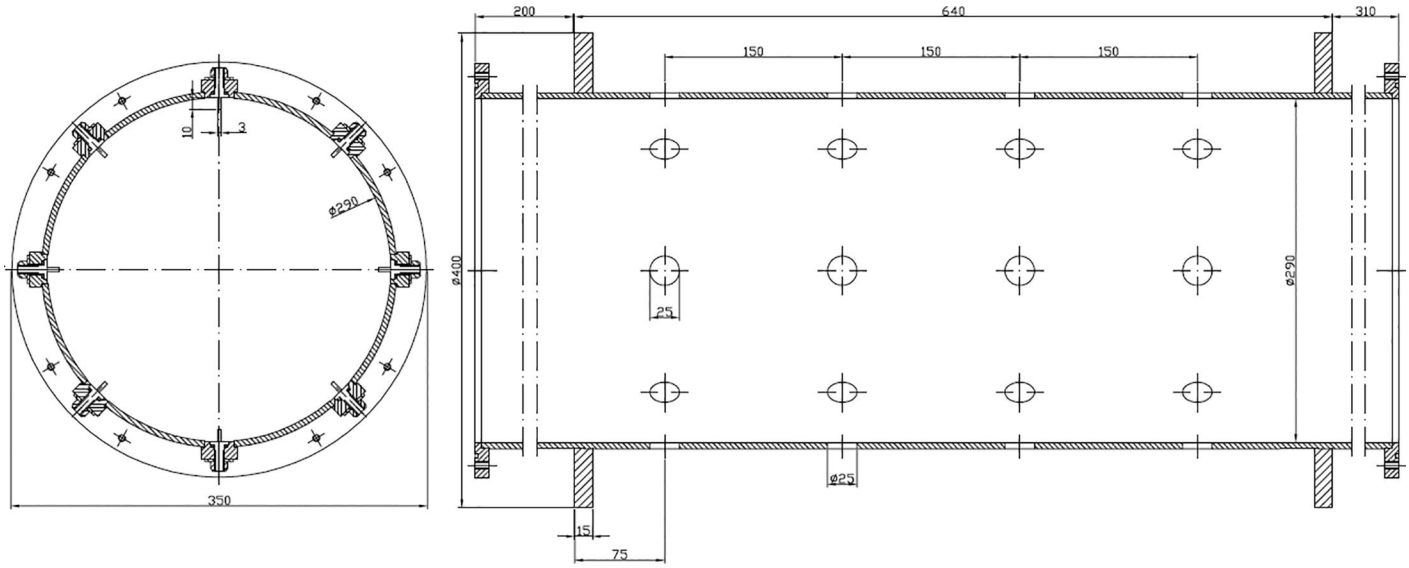

Fig. 1. The rotary drum (horizontal angle 2.5°) with 8 replaceable mixing elements at 4 circumferences used in the experiments.

experimentally based on minimizing the deviations between repetitive measurements. The tracer color was fed in the same manner as the acid. The impulse response was analyzed based on the video frames, as described in section Video Analysis Method Based on Color Saturation.

Residence time distributions were plotted based on acid concentration measurements; see Figure 2. Two repetitions were made for each experiment. At high viscous media, the acid tracer could not be used due to deviations between repetitive experiments. At high viscous media, the acid tracer test results showed no clear trends in the mixing when the mixing conditions were changed.

Video Analysis Method Based on Color Saturation

The impulse response method was used as a basis for developing the video analysis method. The color saturation data from video frames were utilized in obtaining the response from the color tracer impulse.

The measurement videos were shot at full HD resolution, 1920×1080 at 25 frames per second. The video capture was started before the color was applied in the feed of the rotary drum and was continued until the color pulse progressed to the discharge end. The region of interest (ROI), which includes the area where the liquid can be observed, shown in red in Figure 3 (top-left), was manually marked for all videos. The ROI was then cropped

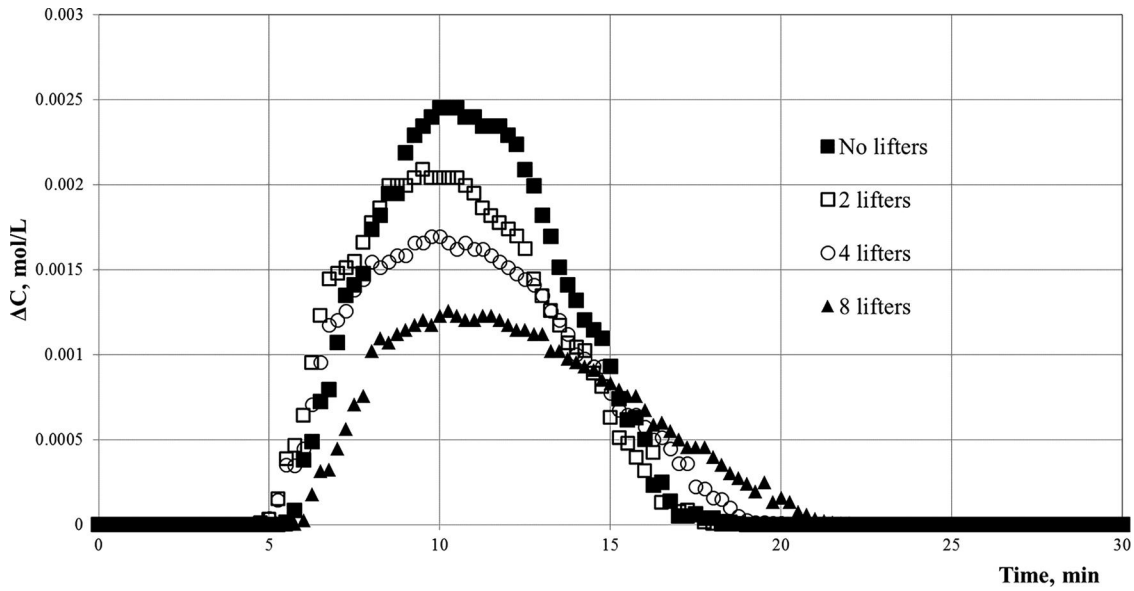

Fig. 2. Acid concentration impulse test in water. RTD for the empty drum, and for 2, 4 and 8 straight lifters on one perimeter (8, 16 and 32 lifters on 4 circumferences) at 2 rpm rotation speed with linear velocity 0.001 m/s.

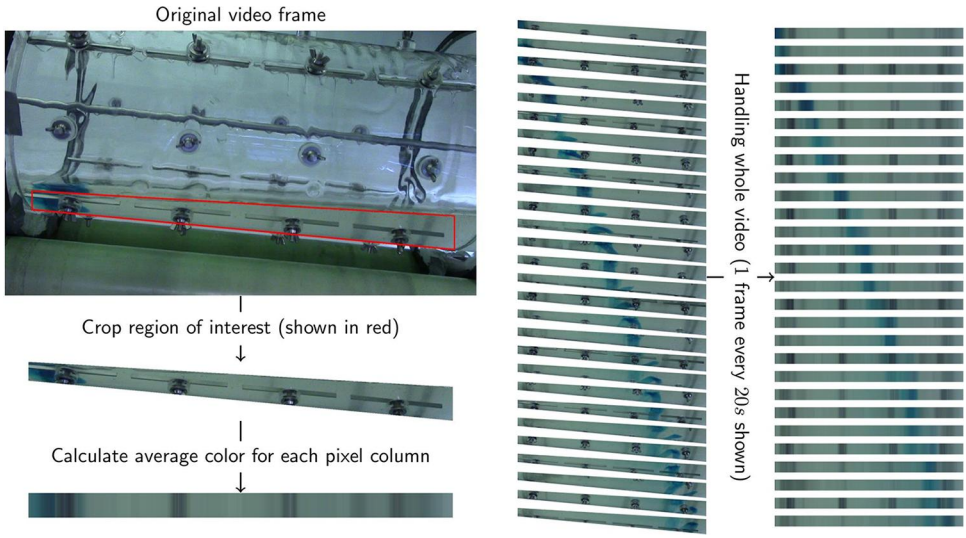

Fig. 3. Diagram of handling separate video frames.

out from each video frame, and, for the ROI, the column-wise average color was calculated. A diagram showing the video analysis method is presented in Figure 5.

In the video processing, each video frame contributes to a one-pixel-high image with the same width as the ROI. These image strips are stacked to form one stack image. The rows in the stack image correspond to sequential chronological video frames. Thus, the color pulse proceeds from left to right as the function of time (top to bottom); see Figure 4 (RGB). To improve the quality of the stack images, they are converted into HSV color space that turns three RGB color components into hue, saturation, and brightness values. The saturation value representing the color concentration or "colorfulness" is used for further processing. The stack images are processed further with a median filter of length 30 s (750 frames) along the time direction to remove dark stripes caused by the lifters and highly saturated spots caused by lifter reflections as shown in Figure 4 (median filtered saturation). The stack image is divided into four areas (see also Figure 5 (right)), and the color saturation values at the boundaries (marked with green lines) located between the lifters are used for calculating further results. The residence time curve is finally plotted from the obtained color saturation values in time series as shown in Figure 5. The residence time distribution from the last mixing zone was used for the evaluation of mixing efficiencies in the drum. This method is unique compared to other image analysis techniques in rotary drum mixing, as they have been concentrated in transverse imaging. The stack images from image strips in video recordings have been utilized, which also differentiates this study from others (Van Puyvelde et al., 1999; Cabaret et al. (2007); Olaofe et al. (2013); Liu and He (2013), Liu et al. (2015), Karali et al. (2016), Santos et al. (2016)). The use of stack images enables the collection of entire mixing volume data at once.

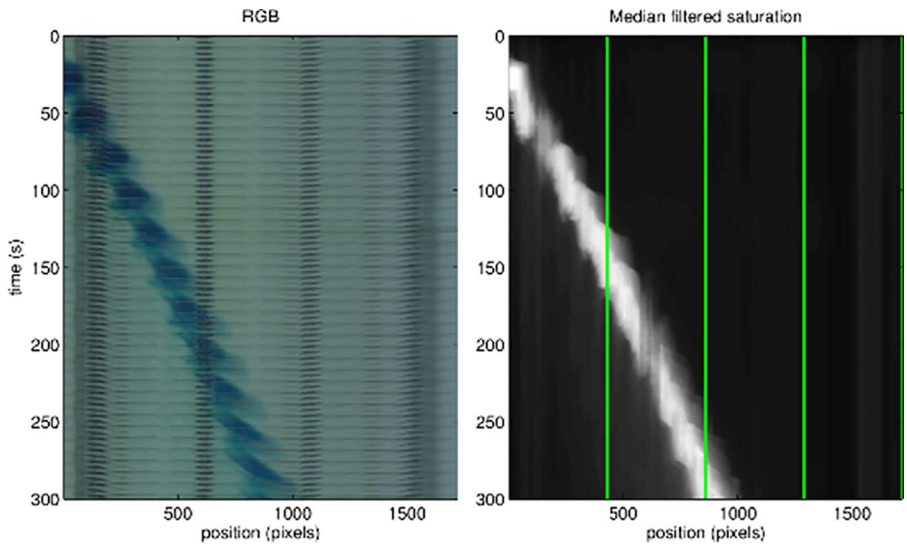

Fig. 4. Stack images showing first 300 s of a measurement video.

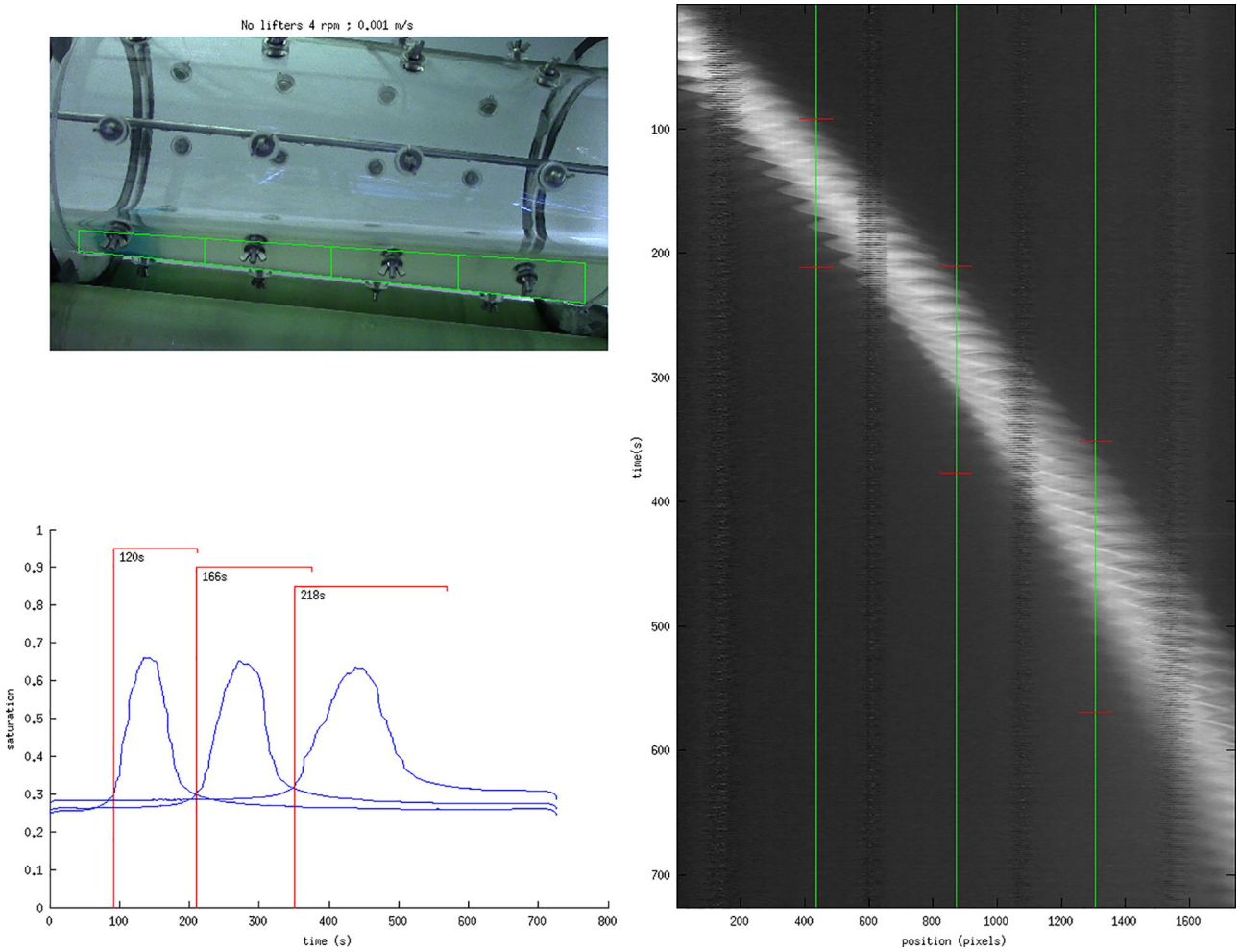

Fig. 5. Video analysis based residence time distributions using the color tracer for the 1% CMC solution at 2 rpm and 0.001 m/s.

Theory and Calculations

Generally, axial mixing in the plug flow reactor can be described with the species transport equation, and it can be used for modeling the residence time distribution as follows:

$$\partial C/\partial t + u\partial C/\partial z = D_i\partial^2 C/\partial z^2 \tag{2}$$

It is noted that the local linear velocity is not exactly constant due to 2.5° horizontal drum angle although average constant velocity is used in Equation (2). The mean residence time and the variance of the residence time are defined as follows:

$$\tau = \int_0^\infty tCdt / \int_0^\infty Cdt \tag{3}$$

$$\sigma^2 = \int_0^\infty (t-)^2 Cdt / \int_0^\infty Cdt \tag{4}$$

Dimensionless dispersion coefficient $D_i/(uz)$ is calculated for large deviation plug flows (Levenspiel, 1999):

$$\sigma_\theta = \sigma^2/\tau = 2D_i/(uz) + 8[D_i/(uz)]^2 \tag{5}$$

Mixedness or the degree of homogeneity is studied with the coefficient of variation (CoV):

$$\mathrm{CoV} = \frac{\sqrt{\frac{\sum_{i=1}^{m}(C_i - C_{AVG})^2}{m-1}}}{C_{AVG}} \tag{6}$$

CoV describes in this case the deviation from the average concentration over the measurement timescale. Axial mixing is more efficient as the CoV approaches zero, which is observed from a flat impulse response. Large CoV values are obtained for nearly ideal plug flows when there is a large deviation from the concentration average, as the Equation (6) is calculated for the whole measurement range.

CoV was computed similarly using the color saturation values (S) from the video processing method, instead of concentration values:

$$\mathrm{CoV_S} = \frac{\sqrt{\frac{\sum_{i=1}^{m}(S_i - S_{AVG})^2}{m-1}}}{S_{AVG}} \tag{7}$$

There are several mixing indices available and, for example, mixing index by Lacey (1954) is adapted here for

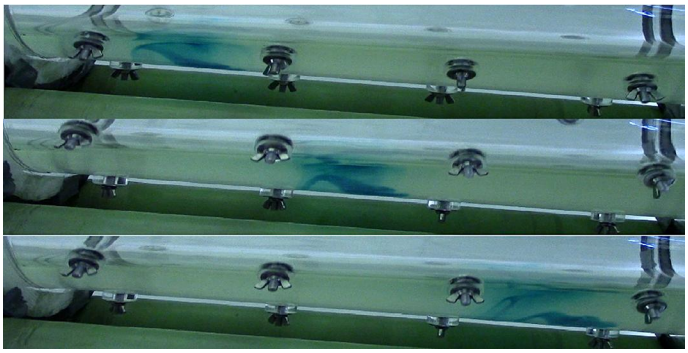

Fig. 6. Video images at 120 s (top), 240 s (middle) and 390 s (bottom) of color tracer travel (1% CMC solution at 2 rpm and 0.001 m/s).

the normalization purposes of closed groups as follows:

$$M = \frac{x_U^2 - x^2}{x_U^2 - x_L^2} \tag{8}$$

Mixing is most efficient among the group under investigation when M is 1.0 in Equation (8). Measured residence time distributions are the raw data for calculating dispersion coefficient from Equation (5) by first calculating the variance and the mean residence time. Integrals in Equations (3) and (4) are calculated from their discretized forms over the measured timescale. The dispersion coefficient is obtained by solving the quadratic Equation (5). Also, the measured residence time distribution is used for the calculation of the coefficient of variation from Equation (6) or Equation (7). Equation (8) is used for ranking different mixing configurations from a closed group based on CoV or dispersion coefficient values. Video image time series from color trace travel in rotary drum is presented in Figure 6.

Results and Discussion

The tip speeds were 0.03 m/s (2 rpm) and 0.06 m/s (4 rpm). The average residence times calculated from average flow velocities were 850 s (0.001 m/s) and 425 s (0.002 m/s). The experiments were performed using water and 1% CMC solution. Nitric acid tracer experiments were done in water for producing traditional residence time distributions, and color tracer experiments were done both for water and for CMC solutions. Color dye was used for acquiring residence time distributions by machine vision based image analysis. The experimental residence time distribution for water with the acid tracer is presented in Figure 2, and the residence time distribution from the video analysis is presented in Figure 5. The experimental setup using acid tracer in water media was evaluated based on the CoV values at 2 rpm and high axial flow velocity 0.002 m/s that were 2.51, 2.50 (no lifters), 2.31, 2.32 (2 straight lifters), 2.15, 2.15 (4 lifters), and 2.04, 2.08 (8 lifters). The CoV values in case of CMC solution without lifters were 4.45, 4.01 (2 rpm and 0.001 m/s), and 4.17, 3.90 (4 rpm and 0.002 m/s). In case of 8 lifters (2 rpm and 0.001 m/s), CoV values were 2.44 and 3.78. For the case of CMC solution, the similar regularity of water experiments could not be observed while increasing lifters due to the deviation of results. A number of tracer fluid experiments in viscous CMC solutions would be necessary to get statistically meaningful results based on these reported experiments. In the case of image analysis for non-Newtonian liquid, the measured repeatability was within ±14% from average CoV, and therefore image analysis method was introduced.

Table I. Mixing indices calculated from dimensionless dispersion coefficient D_i/uz using the data from the acid tracer fluid experiment

	2 rpm, 0.001 m/s	4 rpm, 0.001 m/s	4 rpm, 0.002 m/s
Lifters	***M*, -**	***M*, -**	***M*, -**
	D_i/uz, -	*D_i/uz*, -	*D_i/uz*, -
0	**0.13**	**0.31**	**0**
	0.027	0.034	0.022
2	**0.28**	**0.72**	**0.18**
	0.033	0.05	0.029
4	**0.41**	**0.91**	**0.36**
	0.038	0.058	0.036
8	**0.46**	**1**	**0.46**
	0.04	0.061	0.04

The comparison of lifter configurations between the dimensionless dispersion coefficient and CoV evaluation using the acid impulse response method is presented in Tables I and II. Mixing indices were calculated by substituting x in Equation (8) with dispersion coefficient in Table I. CoV is calculated from Equation (6), which is then used to calculate the mixing index in Equation (8); see Table II. The lifter configurations are ranked almost into identical order using the mixing index values based on the dispersion coefficient or based on CoV from Equation (6). The axial dispersion coefficients were 14–41 cm^2/min for the studied geometries, which are higher compared to Bongo Njeng et al. (2015a) and Gao et al. (2013) results possibly due to different fluid media.

The stack image contains all time frames of horizontal saturation values throughout the drum. The saturation-based residence time distributions were extracted from color tracer test video recordings using image analysis, as explained in section Video Analysis Method Based on Color Saturation. CoV values were calculated using Equation (7) by substituting temporal concentrations with saturation values. The video analysis method was found comparable with acid tracer experiments in

Table II. Mixing indices calculated from coefficient of variation *Co*V using the data from the acid tracer fluid experiment

	2 rpm, 0.001 m/s	4 rpm, 0.001 m/s	4 rpm, 0.002 m/s
Lifters	***M*, -**	***M*, -**	***M*, -**
	CoV, -	*CoV*, -	*CoV*, -
0	**0.7**	**0.82**	**0**
	1.54	1.37	2.5
2	**0.75**	**0.91**	**0.13**
	1.46	1.24	2.32
4	**0.83**	**0.96**	**0.25**
	1.35	1.17	2.15
8	**0.92**	**1**	**0.32**
	1.23	1.12	2.06

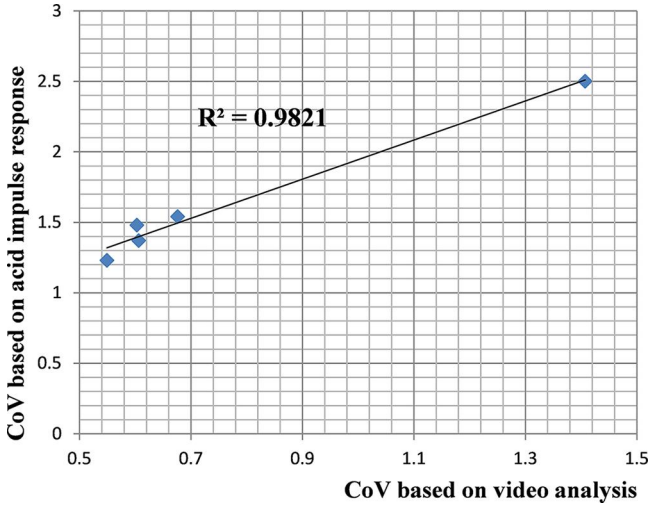

Fig. 7. Comparison of CoV values between the acid impulse and color tracer video analysis.

Table III. The comparison for the ranking of lifter configurations between the acid tracer with concentration response method and the video analysis method for water media. Mixing index calculated from CoV

	Mixing index from acid impulse response method	Mixing index from video analysis method
2 rpm rotational speed, 0.001 m/s flow velocity		
8	1.00	1.00
4	0.82	0.94
No lifters	0.76	0.85
4 rpm rotational speed, 0.001 m/s flow velocity		
No lifters	0.89	0.93
4 rpm rotational speed, 0.002 m/s flow velocity		
No lifters	0.00	0.00

the case of water mixing due to the strong linear dependence ($R^2 = 0.982$); see Figure 7. A monotonic dependence for CoV analyzed with both methods is thus observed. The mixing

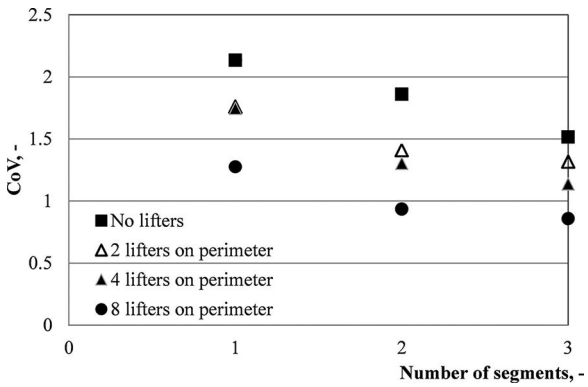

Fig. 8. Local CoV at sequential segments in the rotary drum based on the video analysis method with 1 % CMC-water solution; segment length 0.15 m, tip speed 3 cm/s, and linear flow velocity 0.001 m/s.

Table IV. Mixing indices for lifter configurations with 1% CMC-water solution; segment length 0.15 m, total length from the feed to discharge is 0.85 m

Lifters	2 rpm rotational speed, 0.001 m/s flow velocity
	Mixing index *M*
8	1.00
4	0.63
0	0.20
	Mixing index *M*
	4 rpm rotational speed, 0.001 m/s flow velocity
0	0.12
	Mixing index *M*
	4 rpm rotational speed, 0.002 m/s flow velocity
0	0.00

indices were calculated from Equation (8) using acid impulse response and image analysis methods for the comparison purposes of different mixing configurations. The ranking order of mixing indices is well comparable with acid impulse response and image analysis; see Table III.

The video analysis method allows mixing studies in segments, and the degree of homogenization can be studied in more detail with rotary drums. In the case of 1% CMC-water solution, the number of the local CoV values are presented for the three equal drum segments in Figure 8 at constant drum rotational speed 2 rpm, and 0.001 m/s flow velocity. It should be emphasized that drum lengthwise results for one lifter configuration were obtained from a single experiment due to the block representation of the image analysis method; see also Figure 5. Thus, this method can be used for the analysis of separate mixing zone geometries with non-invasive measurement.

The mixing indices for different configurations for viscous media are presented in Table IV. The comparison was made based on the number of lifters, rotational speeds (or tip speed), and linear velocities (corresponding to mass flow rate). According to the results, the number of lifters and longer residence time increase the axial mixing. The increase of lifters for improving mixing was also noted by Bongo Njeng et al. (2016). The positive effect to axial mixing by increasing residence time or drum length is explained by dispersion time increase (Fogler, 2006).

The proposed image analysis method has operational boundaries as all image analysis methods have. For example, lighting conditions should be adjusted similarly in each experiment, and reflections should be minimized for good video quality.

Conclusions

A new video analysis method for the axial mixing measurement of residence time distributions based on stack images was developed. Hereby, the data is available for the entire mixing volume. The method was applied for comparing mixing efficiencies of different lifter configurations in a pilot rotary drum. Water and CMC solution were used to imitate a diversity of different biological process streams. The video analysis method for the ranking of different mixing configurations was verified against the acid tracer impulse response

method with water experiments. This machine vision based image analysis method in case of high viscous media was used because of the experimental repeatability and because interpretation of results failed in traditional acid tracer experiments. The method enables the determination of instantaneous residence time distributions in multiple blocks. Thus, the proposed method enables the analysis of sequential mixers interaction without sampling or using flow disturbing measurement probes. The rotary drum mixing efficiency was found to increase by increasing number of lifters, residence time, and drum rotational speed.

Nomenclature

C	species concentration, mol/m^3
C_{AVG}	average concentration, mol/m^3
Di	dispersion coefficient, m^2/s
K	consistency index, Pas^{n-1}
M	mixing index, -
m	number of measurements, -
n	power law exponent, -
S	color saturation value, -
S_{AVG}	average color saturation value, -
t	time, s
u	average linear velocity, m/s
x	variable describing the degree of homogeneity, -
x_L	lowest value of closed group describing the degree of homogeneity, -
x_U	highest value of closed group describing the degree of homogeneity, -
z	distance from tracer inlet, m

Greek letters

σ	standard deviation of residence time distribution, -
σ_θ	correlation variance, -
τ	residence time, s

References

Alam, M. A., Mamum, A. A., Qudsieh, I. Y., Muyibi, S. A., and Omar, N. M. (2009). Solid state bioconversion of oil palm empty fruit bunches for cellulase enzyme production using a rotary drum bioreactor, *Biochem. Eng. J.*, **46**, 61–64.

Bongo Njeng, A. S., Vitu, S., Clausse, M., Dirion, J.-L., and Debacq, M. (2015a). Effect of lifter shape and operating parameters on the flow of materials in a pilot rotary kiln: Part I. Experimental RTD and axial dispersion study, *Powder. Tech.*, **269**, 554–565.

Bongo Njeng, A. S., Vitu, S., Clausse, M., Dirion, J.-L., and Debacq, M. (2015b). Effect of lifter shape and operating parameters on the flow of materials in a pilot rotary kiln: Part II. Experimental hold-up and mean residence time modeling, *Powder. Tech.*, **269**, 566–576.

Bongo Njeng, A. S., Vitu, S., Clausse, M., Dirion, J.-L., and Debacq, M. (2016). Effect of lifter shape and operating parameters on the flow of materials in a pilot rotary kiln: Part III. Up-scaling considerations and segregation analysis, *Powder. Tech.*, **297**, 415–428.

Cabaret, F., Bonnot, S., Fradette, L., and Tanguy, P. A. (2007). Mixing time analysis using colorimetric methods and image processing, *Ind. Eng. Chem. Res.*, **46**, 5032–5042.

Fogler, H. S. (2006). *Elements of Chemical Reaction Engineering*, Prentice Hall International, New York, USA.

Gao, Y., Glasser, B. J., Ierapetritou, M. G., Cuitino, A., Muzzio, F. J., Beeckman, J. W., Fassbender, N. A., and Borghard, W. (2013). Measurement of residence time distribution in a rotary calciner, *AIChE. J.*, **59**, 4068–4076.

Ghorbanian, M., Russ, D. C., and Berson, R. E. (2014). Mixing analysis of PCS slurries in horizontal scraped surface reactors, *Bioprocess. Biosyst. Eng.*, **37**, 2113–2119.

Jiang, W. Z., Kitamura, Y., and Li, B. (2005). Improving acidogenic performance in anaerobic degradation of solid organic waste using a rotational drum fermentation system, *Bioresour. Technol.*, **96**, 1537–1543.

Jin, J., Liu, G., Shi, S., and Cong, W. (2010). Studies on the performance of a rotating drum bioreactor for bioleaching processes: Oxygen transfer, solids distribution and power consumption, *Hydrometallurgy.* **103**, 30–34.

Kalamdhad, A. S., and Kazmi, A. A. (2008). Mixed organic waste using rotary drum composter, *Int. J. Environ. Waste. Manag.*, **2**, 24–36.

Karali, M. A., Herz, F., Specht, E., and Mallmann, J. (2016). Comparison of image analysis methods to determine the optimum loading of flighted rotary drums, *Powder. Tech.*, **291**, 147–153.

Lacey, P. M. C. (1954). Developments on the theory of particle mixing, *J. Appl. Chem.*, **4**, 257–268.

Levenspiel, O. (1999). *Chemical Reaction Engineering*, New York: John Wiley & Sons Ltd, New York, USA.

Liu, X., Zhang, C., and Zhan, J. (2015). Quantitative comparison of image analysis methods for particle mixing in rotary drums, *Powder. Tech.*, **282**, 32–36.

Liu, X. Y., and He, L. (2013). Comparison of image-based measuring methods for analysis of particle mixing in rotary drum (Ch. 88), in *Proceedings of the 2012 international conference on information technology and software engineering.* Berlin: Springer-Verlag

Mbaye, S., Dieudé-Fauvel, E., and Baudez, J. C. (2014). Comparative analysis of anaerobically digested wastes flow properties, *Waste. Manag.*, **34**, 2057–2062.

Moeller, G., and Torres, L. G. (1997). Rheological characterization of primary and secondary sludges treated by both aerobic and anaerobic digestion, *Bioresour. Technol.*, **61**, 207–211.

Olaofe, O. O., Buist, K. A., Deen, N. G., van der Hoef, M. A., and Kuipers, J. A. M. (2013). Improved digital image analysis technique for the evaluation of segregation in pseudo-2d beds, *Powder. Tech.*, **244**, 61–74.

Pernenkil, L., and Cooney, C. L. (2006). A review on the continuous blending of powders, *Chem. Eng. Sci.*, **61**, 720–742.

Poole, K. R., Taylor, R. F., and Wall, G. P. (1964). Mixing powders to fine-scale homogeneity: Studies of batch mixing, *I. Chem. Eng-Lond.*, **42**, T305–15.

Porter, H. F., Schurr, G. A., Wells, D. F., and Semrau, K. T. (1973). Solids drying and gas-solid systems in Perry, R. H., Green, D. W., and Maloney, J. O., eds., *Perry's Chemical Engineers' Handbook*, 20–38, Mc Graw-Hill, New York, USA.

Riley, G. L., Tucker, K. G., Paul, G. C., and Thomas, C. R. (2000). Effect of biomass concentration and mycelial morphology on fermentation broth rheology, *Biotechnol. Bioeng.*, **68**, 160–172.

Sajc, L., Grubisic, D., and Vunjic. Novakovic, G. (2000). Bioreactors for plant engineering: An outlook for further research, *Bio. Chem. Eng. J.*, **4**, 89–99.

Šantek, B., Ivancic, B., Horvat, P., Novak, S., and Maric, V. (2006). Horizontal tubular bioreactors in biotechnology, *Chem. Biochem. Eng.*, **20**, 389–399.

Santos, D. A., Duarte, C. R., and Barrozo, M. A. S. (2016). Segregation phenomenon in a rotary drum: Experimentalstudy and CFD simulation, *Powder. Tech.*, **294**, 1–10.

Sherrit, R. G., Chaouki, J., Mehrotra, A. K., and Behie, L. A. (2003). Axial dispersion in the three-dimensional mixing of particles in a rotating drum reactor, *Chem. Eng. Sci.*, **58**, 401–415.

Van Puyvelde, D. R., Young, B. R., Wilson, M. A., and Schmidt, S. J. (1999). Experimental determination of transverse mixing kinetics in a rolling drum by image analysis, *Powder. Tech.*, **106**, 183–191.

Weinekötter, R., and Reh, L. (1995). Continuous mixing of fine particles, *Part Part Syst Char.*, **12**, 46–53.